

Machine learning wildfire susceptibility mapping for Germany

Boris Thies

thies@staff.uni-marburg.de

Philipps-Universität Marburg Fachbereich 19 Geographie <https://orcid.org/0000-0002-0694-3275>

Research Article

Keywords:

Posted Date: November 13th, 2024

DOI: <https://doi.org/10.21203/rs.3.rs-5333357/v1>

License:  This work is licensed under a Creative Commons Attribution 4.0 International License.

[Read Full License](#)

Title: Machine learning wildfire susceptibility mapping for Germany

Author: Boris Thies

Faculty of Geography, Philipps University Marburg, Marburg, Germany

thies@staff.uni-marburg.de

<https://orcid.org/0000-0002-0694-3275>

<https://orcid.org/0000-0002-0694-3275>

Abstract

Wildfires present a significant threat to ecosystems and human life, particularly as global climate change amplifies the likelihood of extreme fire events. This study develops a machine learning-based wildfire susceptibility model for Germany, using data between 2003 and 2023. The primary goal is to identify the dominant wildfire predictors and create monthly susceptibility maps. A Random Forest (RF) algorithm was trained on remote sensing data and a comprehensive set of predictors, including meteorological, terrain, and land cover variables. The results indicate that surface air pressure, elevation, vegetation health, and proximity to urban areas are the most important factors in predicting fire susceptibility. The model achieved 89% accuracy, demonstrating the effectiveness of data-driven approaches in wildfire risk modeling. The monthly susceptibility map for July 2022 highlights northeastern Germany as particularly vulnerable to fire outbreaks. The results offer valuable insights for targeted wildfire prevention and resource allocation, emphasizing the importance of both temporal and spatial dimensions in managing wildfire risks.

1. Introduction

Wildfires, defined as unplanned fires that cause adverse effects on environmental, social, and economic assets (Gill et al., 2013), have significant impacts on human life, ecosystems, and the atmosphere. They contribute to air pollution, destroy forest ecosystems, and exacerbate global warming by releasing carbon stored in vegetation (Bot & Borges, 2022). The role of global climate change in increasing wildfire risks is well recognized. Warmer conditions dry out fuel materials, leading to longer fire seasons, larger burned areas, and a higher likelihood of intense fires (East & Sankey, 2020).

In Europe, individual countries collect and report wildfire statistics, such as fire occurrence, size, and causes. These are aggregated in the Copernicus European Forest Fire Information System (EFFIS), which serves as a key resource for monitoring fire trends and risks. According to EFFIS reports (San-Miguel-Ayanz et al., 2020), there is a notable increase in fire danger levels, with longer fire seasons and more frequent “mega fires”—large, fast-spreading events that exceed traditional firefighting capacities. Importantly, wildfires are no longer a concern limited to Southern Europe but are increasingly threatening central and western Europe.

Rising temperatures and prolonged droughts have made regions such as Germany more susceptible to wildfires. Over the past decade, Germany has experienced some of its warmest years on record, with vegetation stress from drought conditions resulting in canopy cover losses (Mücke & Litvinovitch, 2020; Thonfeld et al., 2022). The country now faces between 400 and 3,000 forest fires annually, affecting up to 5,000 hectares of land (Umweltbundesamt, 2022). As indicated by the German Federal Environment Agency, the probability of fire occurrence is expected to increase in accordance with the projected rise in temperature and decline in precipitation, particularly during the spring, summer, and autumn seasons (Pfeifer et al., 2015; Albert et al., 2015; Lasch-Born et al., 2018).

These developments highlight the urgent need for improved systems of wildfire monitoring, risk prediction, and firefighting resource allocation. Traditional fire risk indices, such as the five-stage forest fire danger index used by the German Weather Service, are based primarily on meteorological conditions (DWD, 2022). However, these models often overlook other crucial fire drivers, such as vegetation conditions and human activity.

Wildfires are initiated when there is an adequate supply of fuel, the fuel is sufficiently dry, the weather is characterized by high temperatures and low humidity, and there is an ignition source present (Bradstock, 2010). These factors are subject to change over time, thereby rendering the prediction of wildfire risk a challenging endeavor. Meteorological conditions exert an influence on the extent of fires, but ignition sources and fuel availability exert a more pronounced influence on the spatial distribution of fires (Clarke et al., 2019; Bar Massada et al., 2013; Pausas & Paula, 2012; Liu et al., 2012; Parisien et al., 2010).

Wildfire behavior is shaped by a combination of meteorological variables, fuel loads, topography, and human factors, all interacting in complex ways (Worsnop et al., 2020). The relationships between these variables are driven by intricate physical processes that are challenging to model accurately (Srock et al., 2018).

Machine learning (ML) techniques present a promising solution for modeling the complexity of wildfire risks. As the availability of data on fire drivers increases, particularly from remote sensing

sources (Forkel et al., 2017), data-driven machine learning models can enhance the accuracy of predictions regarding the occurrence and behavior of wildfires. Jain et al. (2020) provide a comprehensive review of ML applications in this field. The most commonly utilized models include the Random Forest (RF) (e.g., Barreto & Armenteras, 2020; Cao et al., 2017; Jaafari et al., 2019) and neural networks (e.g., Ghorbanzadeh et al., 2019). Other methods, including logistic regression, support vector machines (SVM), and advanced machine learning techniques, have also demonstrated potential for application in wildfire modeling (Bot & Borges, 2022; Bui et al., 2017).

A substantial body of research has employed data-driven machine learning (ML) models to forecast the spatial distribution of wildfire occurrences (Krawchuk et al., 2009; Parisien & Moritz, 2009). Some studies have even extended these predictions beyond the conventional fire season (Bedia et al., 2015; Gudmundsson et al., 2014). Seasonal variations in light, heat, and moisture levels, as well as interannual variability, have a significant impact on wildfire risk (Matin et al., 2017, Sturtevant et al., 2009). However, few studies account for the temporal characteristics of wildfire risk throughout the year (Bakke et al., 2023; Tang et al., 2022; Trucchia et al. 2022).

This study presents the development of a machine learning-based wildfire susceptibility model for Germany, which considers both spatial and temporal dimensions. The primary objectives are to identify the main causes of wildfires and to create cartographic representations of areas that are highly susceptible to such events. Wildfire susceptibility refers to the likelihood of a fire starting in a specific location, based on historical data and environmental factors (Leuenberger et al., 2018). While the term “probability” should not be taken in a strict statistical sense, susceptibility values between 0 and 1 serve as useful indicators for identifying areas at higher risk.

In order to achieve the aforementioned objectives, a satellite-based fire dataset, spanning the period from 2003 to 2023 at a daily temporal resolution, is taken as the target variable. An RF algorithm was used to train the model and identify important factors from a set of weather, terrain, land cover-related, and anthropogenic predictor variables. To account for temporal dynamics, the hydrometeorological and land-cover-related data are analysed on a monthly basis.

Producing accurate wildfire susceptibility maps is a crucial first step in effective wildfire risk management. These maps not only provide insights for current firefighting resource allocation but also pave the way for further risk assessments, such as potential fire intensity and the vulnerability of exposed assets.

This study used freely available data and methods that can be repeated and adapted for other regions..

2. Data and Methods

Table 1 offers an overview of the data employed in this study.

2.1 Data Preprocessing

2.1.1 Fire Data

The target variable for fire risk modeling was based on the “MODIS Collection 6.1 Active Fire Product” (Giglio et al., 2021). The data for Germany (2003–2023) were retrieved from the “Fire Information for Resource Management System” (FIRMS) website. To account for spatially and temporally close fire pixels belonging to the same event, the data were spatially (0.02-degree grid)

105 and temporally (4-day intervals) aggregated by calculating the mean coordinates for each
106 aggregated fire event.

107 **2.1.2 Land Cover Information**

108 The annual global land cover maps from the “Copernicus Climate Change Service” for 2003–2022
109 (2023 data were unavailable) were used for land cover information. To focus on wildfires, the land
110 cover classes were filtered to include forest, shrubland, and grassland, excluding cropland and urban
111 areas.

112 **2.1.3 Hydroclimatic Variables**

113 The climate variables were sourced from the “ERA5 Land” dataset (Muñoz-Sabater et al., 2021) via
114 the Copernicus Climate Data Store. The vapor pressure deficit was computed using the “MetPy”
115 library (May et al., 2022), and the accumulated variables (e.g., precipitation, surface fluxes) were
116 converted to monthly values in accordance with the guidelines set forth by the “European Centre for
117 Medium-Range Weather Forecasts” (<https://confluence.ecmwf.int/>).

118 **2.1.4 Normalized Difference Vegetation Index (NDVI)**

119 Monthly NDVI data at a 1 km resolution were obtained from the “MYD13A3v061” product (Huete
120 et al., 1999). The quality layer provided was used to mask low-quality pixels, thus ensuring the
121 reliability of the vegetation index values.

122 **2.1.5 Land Surface Temperature (LST)**

123 LST data were sourced from the “MYD11A2v061” product (Wan, 1999). The 8-day per-pixel data
124 (1 km resolution) were aggregated into monthly averages. Low-quality pixels were masked out
125 using the included quality layer.

126 **2.1.6 Terrain Information**

127 The digital elevation model (DEM) for Germany was downloaded and used with the GDAL
128 software to calculate additional terrain attributes, including slope and aspect.

129 **2.1.7 Distance to Roads, Railways, Urban areas, and Agricultural Areas**

130 The GDAL “proximity” tool was employed to calculate the distance to roads, railways, settlements,
131 and agricultural areas. Shapefiles for roads and railways were obtained from DIVA-GIS, and land
132 cover maps were used to compute distances to urban and agricultural areas.

133 **2.1.8 Reprojection**

134 In order to extract predictor variables for the fire pixels, all datasets were reprojected in order to
135 align with the MODIS FIRMS dataset's CRS (EPSG 4326). This was achieved through the
136 utilisation of the Python rasterio package.

137 Table 1: Predictor variables considered in the study. The final predictor variables used to model fire susceptibility are
138 highlighted in gray.

Name	Units	Short description	Temporal resolution	Spatial resolution [degree]
10m u-wind	m s ⁻¹	10m eastward wind component	monthly	0.1*0.1
10m v-wind	m s ⁻¹	10m northward wind component	monthly	0.1*0.1
2m dewpoint temperature	K	The temperature at 2 meters that the air must be cooled to reach saturation.	monthly	0.1*0.1
2m temperature	K	Air temperature at 2 meters above the surface	monthly	0.1*0.1
Potential evaporation	m	Potential evaporation	monthly	0.1*0.1
Skin reservoir content	m of water equivalent	The amount of water in the plants and soil.	monthly	0.1*0.1
Skin temperature	K	Land surface temperature	monthly	0.1*0.1
Soil temperature level 1	K	Soil temperature of the soil from 0 to 7 cm depth	monthly	0.1*0.1
Surface latent heat flux	J m ⁻²	Exchange of latent heat between the surface and the atmosphere through turbulent diffusion	monthly	0.1*0.1
Surface net solar radiation	J m ⁻²	Amount of solar radiation reaching the surface minus the amount reflected by the surface	monthly	0.1*0.1
Surface pressure	Pa	pressure of the atmosphere on the land surface	monthly	0.1*0.1
Surface sensible heat flux	J m ⁻²	Exchange of sensible heat between the surface and the atmosphere through turbulent air motion	monthly	0.1*0.1
Total evaporation	m of water equivalent	Accumulated amount of water that has evaporated from the surface	monthly	0.1*0.1
Total precipitation	m	Accumulated liquid and frozen water, including rain and snow, that falls to the surface.	monthly	0.1*0.1
Volumetric soil water layer 1	m ³ m ⁻³	Volume of soil water from 0 to 7 cm depth	monthly	0.1*0.1
Vapor pressure deficit	Pa	Derived from hydrometeorological variables in the ERA5 Land dataset	monthly	0.1*0.1
Height	m	Digital elevation model	static	0.08*0.08
Slope	radians	Derived from digital elevation model	static	0.08*0.08
Aspect	radians	Derived from digital elevation model	static	0.08*0.08
Distance to roads	degrees	Derived from roads shape files	static	0.08*0.08
Distance to rails	degrees	Derived from rails shape files	static	0.08*0.08

139 2.2 Machine Learning Model

140 2.2.1 Dataset Compilation

141 In order to establish meaningful relationships between predictor variables and the occurrence of
142 fire, it is necessary to obtain information about pixels that did not experience fire, in addition to data
143 regarding fire pixels. To this end, the coordinates of each pixel for each year across all relevant land
144 use classes (see above) were extracted. Subsequently, the coordinates of the fire pixels for each
145 month (including a spatial buffer) were matched with those of the aforementioned pixels, and
146 removed from the dataset. This results in a dataset comprising the coordinates of non-fire pixels.
147 Following this, a number of coordinates matching the fire pixels are randomly selected from this
148 dataset, thus enabling the models to learn with a balanced dataset. The procedure is conducted on a
149 monthly basis. Following the preparation of the target and predictor variables, the pixel values of
150 the predictor variables for the fire and non-fire pixel coordinates were extracted and compiled into a
151 final dataset for machine learning. Prior to the training of the model, highly correlated predictor
152 variables were removed (the final predictors are listed in Table 1). The final two years of the dataset
153 were employed as an independent test set (1489 samples). The remaining data (8409 samples) were
154 divided randomly into an 80% training set and a 20% validation set.

155 2.2.2 Model Setup

156 The RF algorithm constructs an ensemble of decision trees, wherein each tree is generated from a
157 bootstrapped sample of the data and splits are based on random subsets of predictors (Breiman,
158 2001). This reduces correlation between trees and improves generalization (Breiman, 2001). The RF
159 model was developed using scikit-learn (Pedregosa et al., 2011). To optimize model performance, a
160 GridSearchCV with 10-fold cross-validation on the training set was conducted (see Table 2). The
161 probability threshold for fire occurrence classification was optimised by maximising model
162 accuracy on the validation set. The final validation was conducted using the independent test data
163 set from the previous two years. To provide a more comprehensive assessment of the model results,
164 a random classifier was employed as a baseline model. The accuracy and F1 score were calculated
165 as validation scores. The importance of the features was estimated using two different approaches:
166 permutation importance and impurity-based importance. The permutation importance was
167 calculated for both the training and test data sets by shuffling the values of each predictor (30
168 random shuffles for each predictor) and observing the resulting reduction in the model's ROC-AUC
169 score. In contrast, impurity-based importance measured the reduction in the classification accuracy
170 introduced by each predictor. To better understand the relationship between predictor variables and
171 fire risk, partial dependence plots were generated, showing the marginal effect of each predictor on
172 fire risk while holding other variables constant. Ultimately, a fire susceptibility map was generated
173 for July 2022 using the predicted probabilities from the RF model.

174

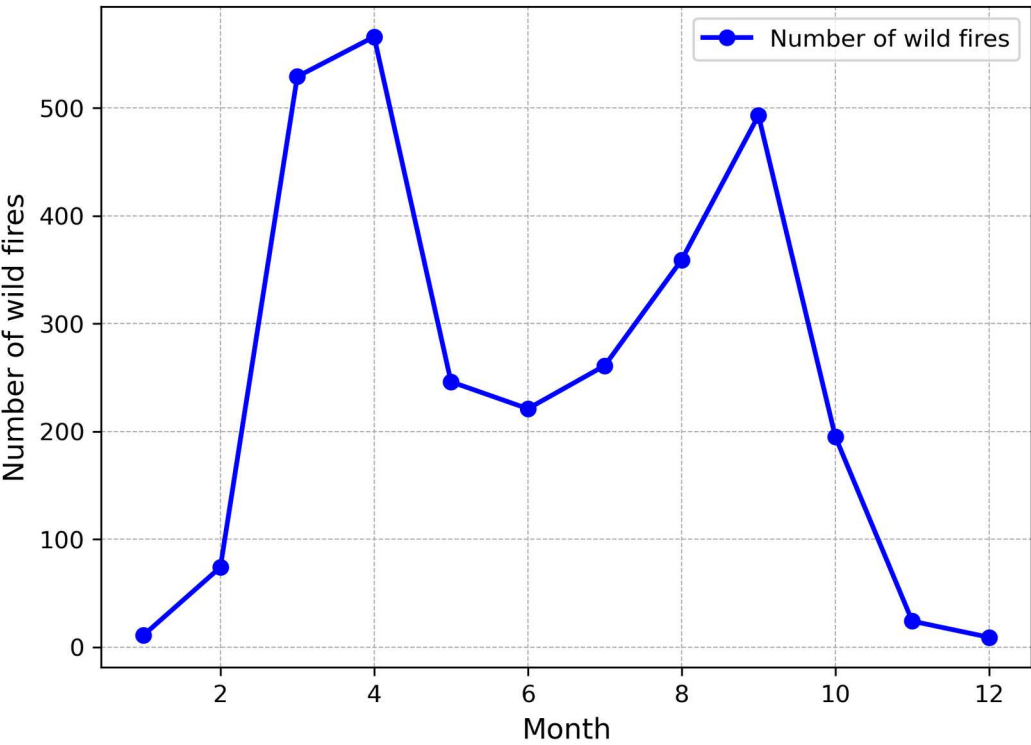
175 Table 2: Parameters and values taken into account for hyperparameter tuning. For a detailed explanation of the
176 parameters, see link <https://scikit-learn.org/stable/modules/generated/sklearn.ensemble.RandomForestClassifier.html>.

Parameter	Range	Best value
n_estimators	100, 200, 300, 400, 500	300
max_features	auto, sqrt, log2, None	sqrt
max_depth	None, 10, 20, 30, 40, 50	30
min_samples_split	2, 5, 10, 20	2
min_samples_leaf	1, 2, 4, 10	1
bootstrap	True, False	0

177 **3. Results and Discussion**

178 **3.1 Monthly Fire Events**

179 The distribution of monthly fire events in Germany from 2003 to 2023 (Figure 1) reveals distinct
180 seasonal patterns. Wildfires are most frequent between March and October, with peaks in April and
181 September. This seasonal trend aligns with known environmental variations, particularly
182 temperature and vegetation moisture. The decrease in fire occurrences from May to July may be
183 attributed to increased vegetation moisture during these months, while the rise in fires from August
184 to September is likely driven by late-summer dryness. The prominence of wildfire events in both
185 early spring and late summer underscores the importance of targeted fire management strategies
186 during these critical periods. As Modugno et al. (2016) suggests, fire prevention efforts, resource
187 allocation, and public awareness campaigns should be concentrated in these high-risk months to
188 mitigate fire damage.



189
190 Figure 1: Number of fires detected per month for Germany in the study period 2003 to 2023.

3.2 Annual Wildfire Trends

A clear upward trend in wildfire incidents has been observed since 2017, with a significant peak in 2018 (Figure 2). This increase in fire frequency correlates with rising temperatures and prolonged droughts, a pattern consistent with climate change projections (Abatzoglou et al., 2016). While fire occurrences between 2003 and 2010 remained relatively low and stable, fluctuating between 50 and 150 events annually, the period from 2010 onwards witnessed a steady rise, likely driven by increasingly hotter and drier summers. The slight decline in fire activity in 2021 may be attributed to temporary climatic variations or improvements in fire management practices. However, the overall trend indicates a growing wildfire threat, consistent with broader European trends (Gudmundsson et al., 2014). This long-term increase in wildfire frequency suggests that Germany, like other regions, is experiencing climate-induced shifts in fire regimes, with hotter and drier conditions leading to more frequent and intense wildfires (Bowman et al., 2020).

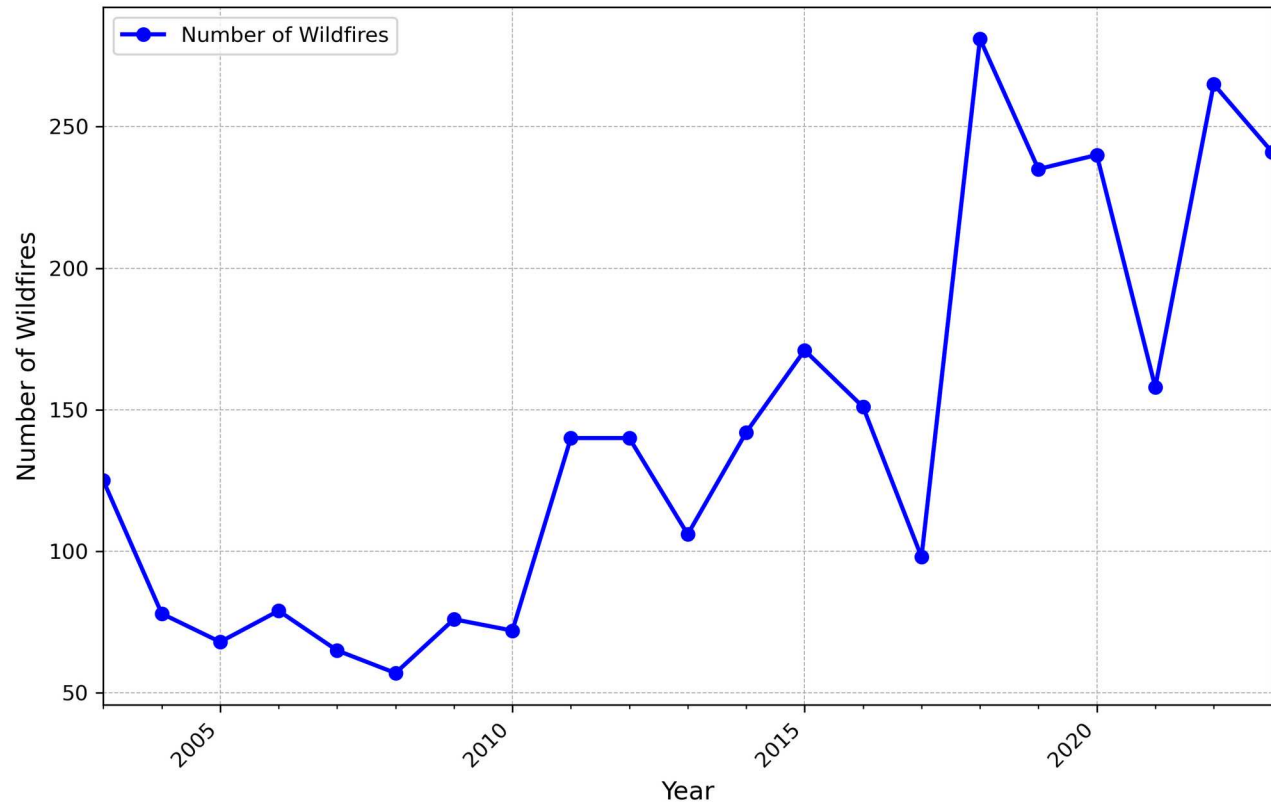


Figure 2: Temporal development of the number of detected fires per year in Germany.

3.3 Model Accuracy and Threshold Analysis

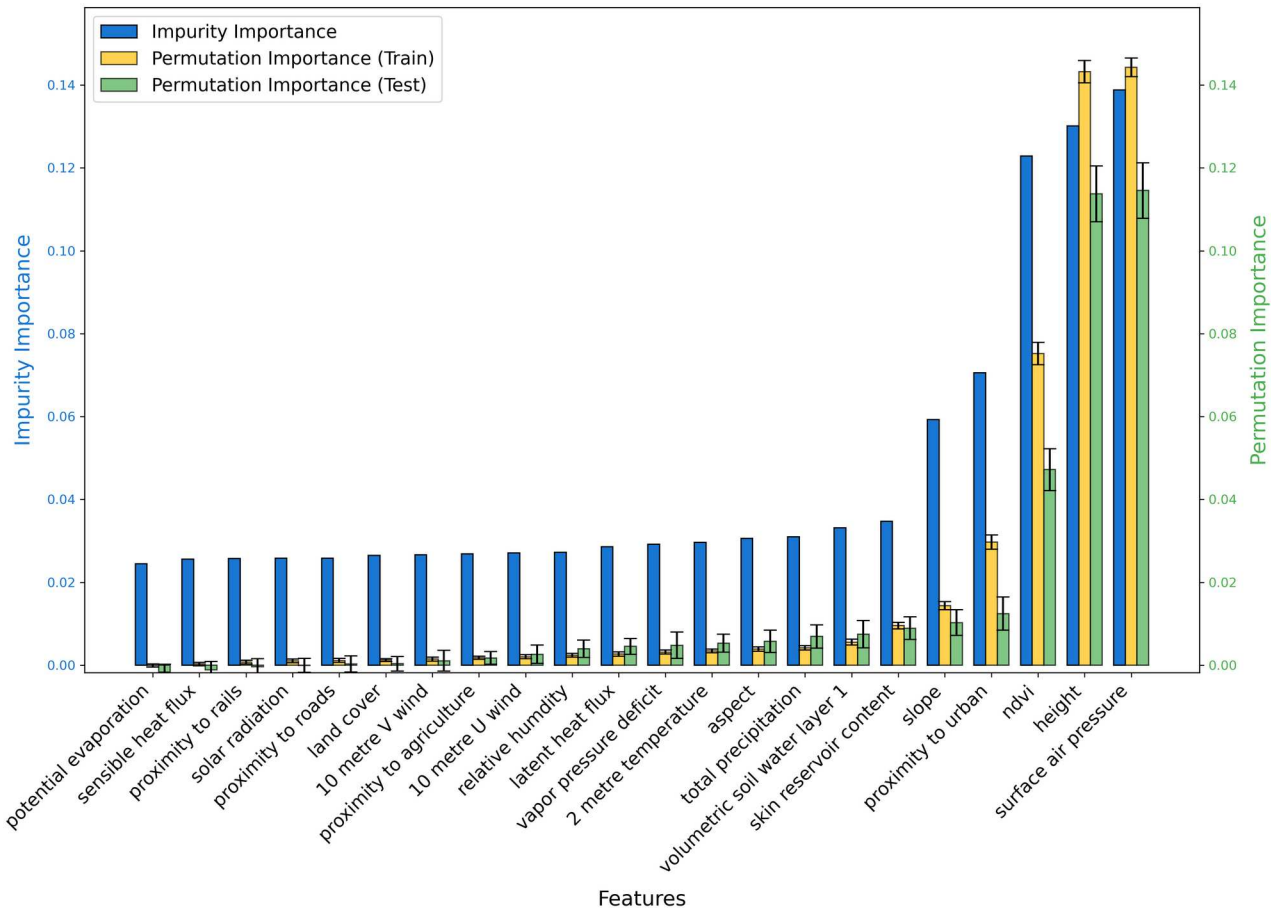
The Random Forest model achieved its highest accuracy (90%) at a probability threshold of 0.46. This threshold effectively balances sensitivity and specificity in detecting wildfires. As the threshold increases beyond 0.6, accuracy declines, indicating that the model becomes overly conservative and misses more fire events. This trade-off between false positives and false negatives is a common challenge in fire risk modeling (Schoennagel et al., 2017). In critical fire-prone areas where the cost of missing a fire event is higher than that of false alarms, a lower probability threshold may be advisable. This approach can enhance decision-making in fire detection and resource deployment. Table 3 illustrates the validation results with the independent data set from 2022 to 2023, presented in comparison with the random baseline classifier.

215 Table 3: Validation results with the independent test data set from 2022 to 2023.

	Random Forest Classifier	Random Baseline Classifier
Accuracy	0.83	0.6
F1 Score	0.69	0.34

216 **3.4 Feature Importance**

217 The most important predictors of fire susceptibility in the model were surface air pressure,
218 elevation, NDVI, and proximity to urban areas (Figure 3). Higher surface air pressure is associated
219 with dry, stable weather conditions that promote fire ignition and spread, while lower elevation
220 areas, which are often closer to human activity and denser vegetation, exhibit greater fire
221 susceptibility. NDVI, a proxy for vegetation health, is inversely related to fire risk, with lower
222 NDVI values indicating stressed or sparse vegetation that is more prone to burning (Modugno et al.,
223 2016). The proximity to urban areas further emphasizes the role of human-caused ignitions, as
224 documented in studies by Zambon et al. (2019) and Vilar et al. (2010). The greater proportion of the
225 dynamic meteorological predictors demonstrate low importance, both in terms of impurity with
226 respect to the training data and with regard to the permutation for training and testing. Nevertheless,
227 the low significance does not necessarily indicate that the relevant predictors exert no influence on
228 the favourable model result. Rather, they play a significant role when considered collectively and in
229 interaction with other predictors, contributing to the overall result of the model (Rew et al. 2023,
230 Wu et al. 2023).



231
232 Figure 3: Feature importances of the predictor variables that were considered in the final RF model.

3.5 Partial Dependence Plots

The partial dependence plots (Figure 4) provide deeper insight into how specific predictor variables influence fire risk for the four most important predictor variables. For surface air pressure, height and NDVI, a discernible and meaningful correlation with fire susceptibility can be observed. The occurrence of high-pressure weather conditions is associated with elevated levels of fire susceptibility. Areas situated in close proximity to human settlements and exhibiting low NDVI values are characterised by elevated fire susceptibility values. Low-elevation areas, often near human settlements and with denser vegetation, are particularly vulnerable to fire outbreaks (e.g. Archibald et al., 2009). The inverse relationship between NDVI and fire susceptibility provides further evidence of the role of vegetation health in wildfire prediction. Healthy vegetation is less prone to fires (Bowman et al., 2020). Similarly, the slight positive correlation between proximity to urban areas and fire risk highlights the impact of human activity on fire ignition (Vilar et al., 2010; Zambon et al., 2019).

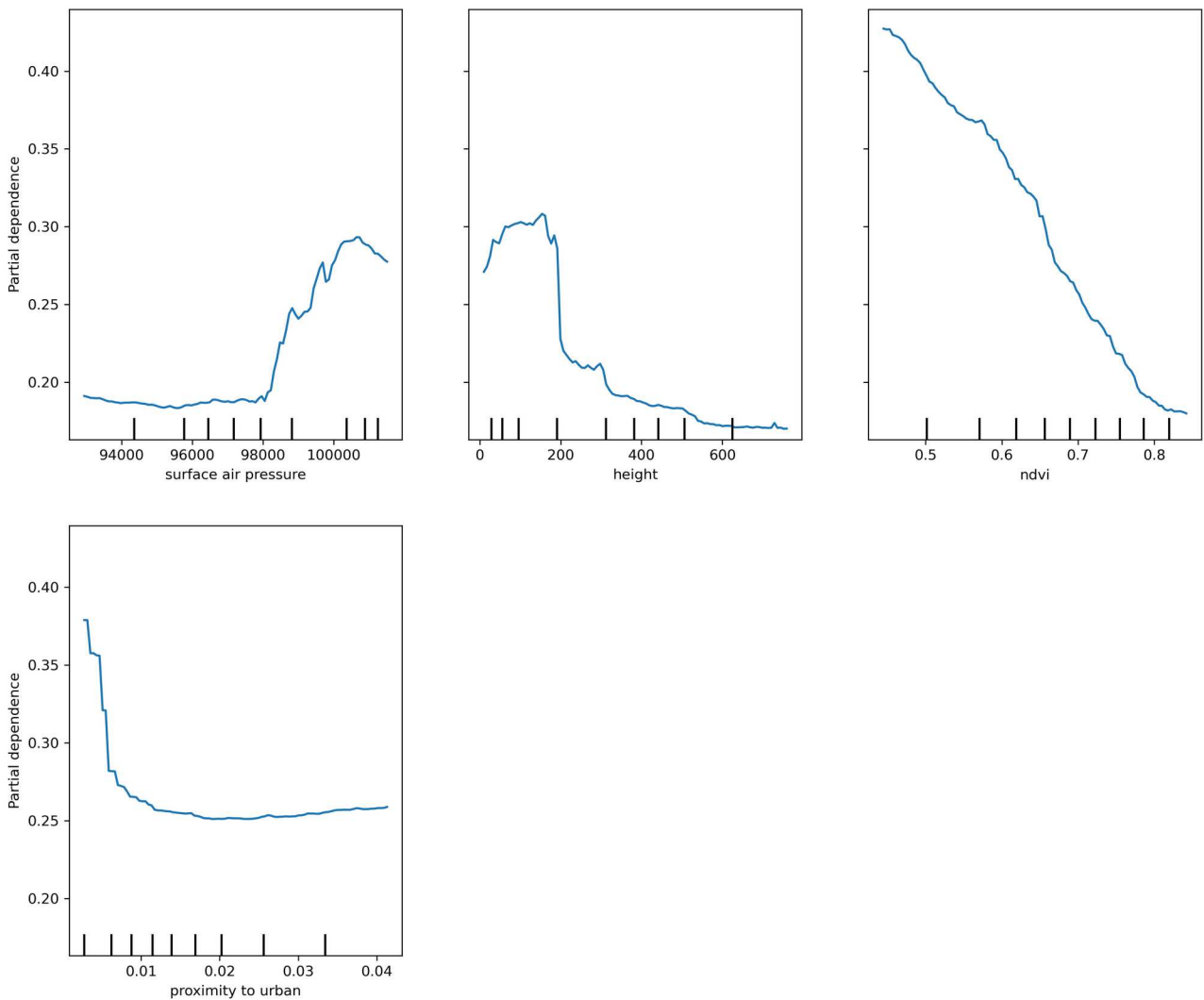
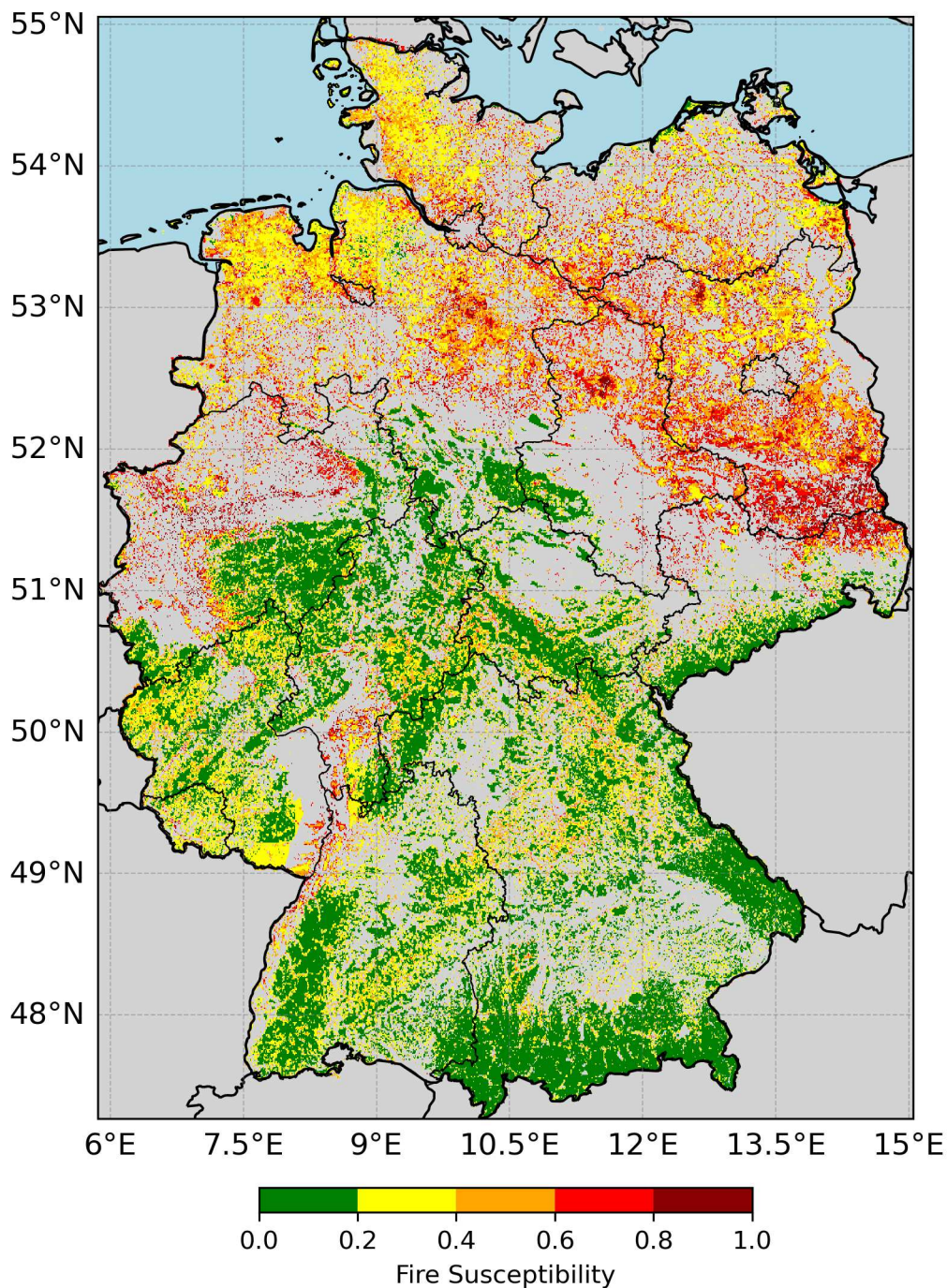


Figure 4: Partial dependence plots for the four most important predictor variables.

3.6 Fire Susceptibility Map

The fire susceptibility map for July 2022 (Figure 5) identifies northeastern Germany, particularly Brandenburg and Saxony-Anhalt, as high-risk areas for wildfires. These regions are characterised

251 by dry summers, sandy soils, and extensive pine forests, all of which contribute to elevated fire risk.
 252 Interestingly, southern Germany, particularly Bavaria and Baden-Württemberg, exhibits lower fire
 253 susceptibility probably due to more favorable climatic conditions and land-use patterns. Higher
 254 precipitation and denser vegetation in these regions might reduce wildfire potential during the
 255 summer months. The influence of human activity is also evident, particularly in urban-adjacent
 256 areas like the Rhine-Main region, where proximity to settlements increases fire risk.



257
 258 *Figure 5: Fire susceptibility map for July 2022 predicted by the created RF model.*

259 **4. Conclusion**

260 This study demonstrates the potential of machine learning techniques, specifically Random Forest
261 algorithms, to enhance wildfire susceptibility modeling in Germany. By integrating spatial and
262 temporal data, the model effectively identifies key wildfire risk predictors and generates accurate
263 monthly susceptibility maps. The findings show that surface air pressure, elevation, vegetation
264 health (NDVI), and proximity to urban areas are crucial factors influencing wildfire occurrence,
265 highlighting the complex interplay of meteorological, topographical, and ecological variables. The
266 susceptibility maps, especially for high-risk months like July 2022, provide essential insights for
267 resource allocation and fire prevention strategies. As climate change continues to increase the
268 frequency and severity of wildfires, this model offers a flexible and scalable tool for future risk
269 assessment. Further research should consider incorporating additional dynamic predictors and
270 refining the temporal resolution to enhance early warning systems and disaster preparedness.

271 **Acknowledgment**

272 The author greatly acknowledges all data providers. The “ERA5-Land” and land cover maps were
273 sourced from the “Copernicus Climate Change Service (C3S) Climate Data Store”, while the NDVI
274 and LST data were obtained from “NASA's Land Processes Distributed Active Archive Center (LP
275 DAAC)”. The digital elevation model was obtained from the Federal Agency for Cartography and
276 Geodesy and the shape files for roads and railways were downloaded from DIVA-GIS.

277 **Competing Interests**

278 The authors have no relevant financial or non-financial interests to disclose.

279 **References**

- 280 Abatzoglou JT, Williams AP. Impact of anthropogenic climate change on wildfire across western
281 US forests. *Proceedings of the National Academy of sciences*. 2016;113(42):11770–5.
- 282 Albert M, Hansen J, Nagel J, Schmidt M, Spellmann H. Assessing risks and uncertainties in forest
283 dynamics under different management scenarios and climate change. *Forest Ecosystems*. 2015;2:1–
284 21.
- 285 Archibald S, Roy DP, van Wilgen BW, Scholes RJ. What limits fire? An examination of drivers of
286 burnt area in Southern Africa. *Global Change Biology*. 2009;15(3):613–30.
- 287 Bakke SJ, Wanders N, Van Der Wiel K, Tallaksen LM. A data-driven model for Fennoscandian
288 wildfire danger. *Natural hazards and earth system sciences*. 2023;23(1):65–89.
- 289 Barreto JS, Armenteras D. Open data and machine learning to model the occurrence of fire in the
290 ecoregion of “Llanos Colombo–Venezolanos.” *Remote Sensing*. 2020;12(23):3921.
- 291 Bedia J, Herrera S, Gutiérrez JM, Benali A, Brands S, Mota B, et al. Global patterns in the
292 sensitivity of burned area to fire-weather: Implications for climate change. *Agricultural and Forest*
293 *Meteorology*. 2015;214:369–79.
- 294 Bedia J, Herrera S, Gutiérrez JM, Benali A, Brands S, Mota B, et al. Global patterns in the
295 sensitivity of burned area to fire-weather: Implications for climate change. *Agricultural and Forest*
296 *Meteorology*. 2015;214:369–79.

297 Bot K, Borges JG. A systematic review of applications of machine learning techniques for wildfire
 298 management decision support. *Inventions*. 2022;7(1):15.

299 Bowman DM, Kolden CA, Abatzoglou JT, Johnston FH, van der Werf GR, Flannigan M. Vegetation
 300 fires in the Anthropocene. *Nature Reviews Earth & Environment*. 2020;1(10):500–15.

301 Bradstock RA. A biogeographic model of fire regimes in Australia: current and future implications.
 302 *Global Ecology and Biogeography*. 2010;19(2):145–58.

303 Bradstock R, Penman T, Boer M, Price O, Clarke H. Divergent responses of fire to recent warming
 304 and drying across south-eastern Australia. *Global Change Biology*. 2014;20(5):1412–28.

305 Breiman L. Random forests. *Machine learning*. 2001;45:5–32.

306 Bui DT, Bui QT, Nguyen QP, Pradhan B, Nampak H, Trinh PT. A hybrid artificial intelligence
 307 approach using GIS-based neural-fuzzy inference system and particle swarm optimization for forest
 308 fire susceptibility modeling at a tropical area. *Agricultural and forest meteorology*. 2017;233:32–44.

309 Cao Y, Wang M, Liu K. Wildfire susceptibility assessment in Southern China: A comparison of
 310 multiple methods. *International Journal of Disaster Risk Science*. 2017;8:164–81.

311 Clarke H, Gibson R, Cirulis B, Bradstock RA, Penman TD. Developing and testing models of the
 312 drivers of anthropogenic and lightning-caused wildfire ignitions in south-eastern Australia. *Journal*
 313 *of environmental management*. 2019;235:34–41.

314 Deutscher Wetterdienst - Übersicht - Erläuterungen zum Waldbrandgefahrenindex [Internet]. [cited
 315 2024 Oct 9]. Available from:
 316 [https://www.dwd.de/DE/fachnutzer/landwirtschaft/dokumentationen/allgemein/
 317 basis_waldbrandgefahrenindex_doku.html;jsessionid=8E5B6B82756F857D0FEBED65B2AF1939.
 318 live21071?nn=344238](https://www.dwd.de/DE/fachnutzer/landwirtschaft/dokumentationen/allgemein/basis_waldbrandgefahrenindex_doku.html;jsessionid=8E5B6B82756F857D0FEBED65B2AF1939.live21071?nn=344238)

319 Dos Santos AC, da Rocha Montenegro S, Ferreira MC, Barradas ACS, Schmidt IB. Managing fires
 320 in a changing world: Fuel and weather determine fire behavior and safety in the neotropical
 321 savannas. *Journal of environmental management*. 2021;289:112508.

322 East AE, Sankey JB. Geomorphic and sedimentary effects of modern climate change: current and
 323 anticipated future conditions in the western United States. *Reviews of Geophysics*.
 324 2020;58(4):e2019RG000692.

325 Forkel M, Dorigo W, Lasslop G, Teubner I, Chuvieco E, Thonicke K. A data-driven approach to
 326 identify controls on global fire activity from satellite and climate observations (SOFIA V1).
 327 *Geoscientific Model Development*. 2017;10(12):4443–76.

328 Ghorbanzadeh O, Blaschke T, Gholamnia K, Aryal J. Forest fire susceptibility and risk mapping
 329 using social/infrastructural vulnerability and environmental variables. *Fire*. 2019;2(3):50.

330 Giglio L, Schroeder W, Hall JV, Justice CO. MODIS Collection 6 and Collection 6.1 Active Fire
 331 Product User’s Guide. National Aeronautical and Space Administration—NASA: Washington, DC,
 332 USA. 2021;64.

333 Gill AM, Stephens SL, Cary GJ. The worldwide “wildfire” problem. *Ecological applications*.
 334 2013;23(2):438–54.

335 Gudmundsson L, Rego FC, Rocha M, Seneviratne SI. Predicting above normal wildfire activity in
 336 southern Europe as a function of meteorological drought. *Environmental Research Letters*.
 337 2014;9(8):084008.

338 Huang F, Shangguan W, Li Q, Li L, Zhang Y. Beyond prediction: An integrated post-hoc approach
339 to interpret complex model in hydrometeorology. *Environmental Modelling & Software*.
340 2023;167:105762.

341 Huete A, Justice C, Van Leeuwen W. MODIS vegetation index (MOD13). Algorithm theoretical
342 basis document. 1999;3(213):295–309.

343 Jaafari A, Zenner EK, Panahi M, Shahabi H. Hybrid artificial intelligence models based on a neuro-
344 fuzzy system and metaheuristic optimization algorithms for spatial prediction of wildfire
345 probability. *Agricultural and forest meteorology*. 2019;266:198–207.

346 Jain P, Coogan SC, Subramanian SG, Crowley M, Taylor S, Flannigan MD. A review of machine
347 learning applications in wildfire science and management. *Environmental Reviews*.
348 2020;28(4):478–505.

349 Krawchuk MA, Moritz MA, Parisien MA, Van Dorn J, Hayhoe K. Global pyrogeography: the
350 current and future distribution of wildfire. *PloS one*. 2009;4(4):e5102.

351 Lasch-Born P, Suckow F, Gutsch M, Hauf Y, Hoffmann P, Kollas C, et al. Fire, late frost, nun moth
352 and drought risks in Germany's forests under climate change. 2016;

353 Leuenberger M, Parente J, Tonini M, Pereira MG, Kanevski M. Wildfire susceptibility mapping:
354 Deterministic vs. stochastic approaches. *Environmental Modelling & Software*. 2018;101:194–203.

355 Liu Z, Yang J, Chang Y, Weisberg PJ, He HS. Spatial patterns and drivers of fire occurrence and its
356 future trend under climate change in a boreal forest of Northeast China. *Global Change Biology*.
357 2012;18(6):2041–56.

358 Massada AB, Syphard AD, Stewart SI, Radeloff VC. Wildfire ignition-distribution modelling: a
359 comparative study in the Huron–Manistee National Forest, Michigan, USA. *International journal of*
360 *wildland fire*. 2012;22(2):174–83.

361 Massada AB, Syphard AD, Stewart SI, Radeloff VC. Wildfire ignition-distribution modelling: a
362 comparative study in the Huron–Manistee National Forest, Michigan, USA. *International journal of*
363 *wildland fire*. 2012;22(2):174–83.

364 Matin MA, Chitale VS, Murthy MS, Uddin K, Bajracharya B, Pradhan S. Understanding forest fire
365 patterns and risk in Nepal using remote sensing, geographic information system and historical fire
366 data. *International journal of wildland fire*. 2017;26(4):276–86.

367 May RM, Goebbert KH, Thielen JE, Leeman JR, Camron MD, Bruick Z, et al. MetPy: A
368 meteorological Python library for data analysis and visualization. *Bulletin of the American*
369 *Meteorological Society*. 2022;103(10):E2273–84.

370 Modugno S, Balzter H, Cole B, Borrelli P. Mapping regional patterns of large forest fires in
371 Wildland–Urban Interface areas in Europe. *Journal of environmental management*. 2016;172:112–
372 26.

373 Mücke HG, Litvinovitch JM. Heat extremes, public health impacts, and adaptation policy in
374 Germany. *International journal of environmental research and public health*. 2020;17(21):7862.

375 Muñoz-Sabater J, Dutra E, Agustí-Panareda A, Albergel C, Arduini G, Balsamo G, et al. ERA5-
376 Land: A state-of-the-art global reanalysis dataset for land applications. *Earth system science data*.
377 2021;13(9):4349–83.

378 Parisien MA, Miller C, Ager AA, Finney MA. Use of artificial landscapes to isolate controls on
379 burn probability. *Landscape Ecology*. 2010;25:79–93.

380 Parisien MA, Moritz MA. Environmental controls on the distribution of wildfire at multiple spatial
381 scales. *Ecological Monographs*. 2009;79(1):127–54.

382 Pausas JG, Paula S. Fuel shapes the fire–climate relationship: evidence from Mediterranean
383 ecosystems. *Global Ecology and Biogeography*. 2012;21(11):1074–82.

384 Pedregosa F, Varoquaux G, Gramfort A, Michel V, Thirion B, Grisel O, et al. Scikit-learn: Machine
385 learning in Python. *the Journal of machine Learning research*. 2011;12:2825–30.

386 Penman T, Collins L, Price O, Bradstock RA, Metcalf S, Chong D. Examining the relative effects of
387 fire weather, suppression and fuel treatment on fire behaviour—A simulation study. *Journal of*
388 *environmental management*. 2013;131:325–33.

389 Pfeifer S, Bülow K, Gobiet A, Hänsler A, Mudelsee M, Otto J, et al. Robustness of ensemble
390 climate projections analyzed with climate signal maps: seasonal and extreme precipitation for
391 Germany. *Atmosphere*. 2015;6(5):677–98.

392 San-miguel-ayanz J, Durrant T, Boca R, Liberta G, Branco A, De R, et al. Advance EFFIS report on
393 Forest Fires in Europe, Middle East and North Africa 2017. 2020;

394 Schoennagel T, Balch JK, Brenkert-Smith H, Dennison PE, Harvey BJ, Krawchuk MA, et al. Adapt
395 to more wildfire in western North American forests as climate changes. *Proceedings of the National*
396 *Academy of Sciences*. 2017;114(18):4582–90.

397 Srock AF, Charney JJ, Potter BE, Goodrick SL. The hot-dry-windy index: A new fire weather index.
398 *Atmosphere*. 2018;9(7):279.

399 Sturtevant BR, Scheller RM, Miranda BR, Shinneman D, Syphard A. Simulating dynamic and
400 mixed-severity fire regimes: a process-based fire extension for LANDIS-II. *Ecological Modelling*.
401 2009;220(23):3380–93.

402 Tang X, Machimura T, Li J, Yu H, Liu W. Evaluating seasonal wildfire susceptibility and wildfire
403 threats to local ecosystems in the largest forested area of China. *Earth’s Future*.
404 2022;10(5):e2021EF002199.

405 Thonfeld F, Gessner U, Holzwarth S, Kriese J, Da Ponte E, Huth J, et al. A first assessment of
406 canopy cover loss in Germany’s forests after the 2018–2020 drought years. *Remote Sensing*.
407 2022;14(3):562.

408 Trucchia A, Meschi G, Fiorucci P, Gollini A, Negro D. Defining wildfire susceptibility maps in Italy
409 for understanding seasonal wildfire regimes at the national level. *Fire*. 2022;5(1):30.

410 Umweltbundesamt; 2013 [cited 2024 Oct 9]. Waldbrände. Available from:
411 <https://www.umweltbundesamt.de/daten/land-forstwirtschaft/waldbraende>

412 Vilar L, Woolford DG, Martell DL, Martín MP. A model for predicting human-caused wildfire
413 occurrence in the region of Madrid, Spain. *International Journal of Wildland Fire*. 2010;19(3):325–
414 37.

415 Wan Z. MODIS land-surface temperature algorithm theoretical basis document (LST ATBD).
416 Institute for Computational Earth System Science, Santa Barbara. 1999;75:18.

417 Worsnop RP, Scheuerer M, Hamill TM. Extended-range probabilistic fire-weather forecasting based
418 on ensemble model output statistics and ensemble copula coupling. *Monthly Weather Review*.
419 2020;148(2):499–521.

420 Wu G, Zhang J, Xue H. Long-Term Prediction of Hydrometeorological Time Series Using a PSO-
421 Based Combined Model Composed of EEMD and LSTM. *Sustainability*. 2023;15(17):13209.

422 Zambon I, Cerdà A, Cudlin P, Serra P, Pili S, Salvati L. Road network and the spatial distribution of
423 wildfires in the Valencian community (1993–2015). *Agriculture*. 2019;9(5):100.

424